Journal of Computer Assisted Tomography
11(1):24–30, January/February

Rapid Three-Dimensional Angiography with Undersampled MR Imaging

Van J. Wedeen and Yong Sheng Chao

Abstract: Techniques for subtraction angiography with magnetic resonance imaging have been extended from two to three dimensions, and a novel method that reduces the expected data acquisition time by at least an order of magnitude is presented. Electrocardiogram-gated three-dimensional (3D) images are acquired by Fourier transform technique, and flow contrast is obtained by subtracting pairs of images acquired at different points in the cardiac cycle. The vascular tree is shown in 3D perspective by means of a surface detection and a 3D display program. Isotropic 3D angiography requires determining the disposition of the blood vessels in a matrix of cubical voxels. Using orthodox Fourier transform technique, for an image matrix with 256 voxels to the edge, a data acquisition with 256 × 256 = 65 K phase-encodings would be needed. If gated, this would require ~1 day. In this study we abbreviate the data acquisition by doing only 1/64 of the usual set of phase-encoding gradient pulses. Spatial resolution is undiminished, but aliasing or "wraparound" results in each of the two phase-encoded coordinates of the 3D image. This aliasing is rectified in a two stage process. First, 64 copies of the undersampled 3D arteriogram are juxtaposed in a two-dimensional grid pattern. This assembles many copies of the complete vascular tree. Because they occupy only a small fraction of ambient volume, these copies are unlikely to overlap or collide with one another. Second, a single copy of the vascular tree is isolated by a surface detection program that takes advantage of the fact that the vascular tree is topologically connected. Studies of the abdominal aorta are presented. **Index Terms:** Magnetic resonance imaging, techniques—Blood, flow dynamics—Angiography.

Methods for angiography with magnetic resonance (MR) imaging have recently been published (1,2). These methods use the distinctive signal characteristics of moving protons to selectively enhance the signal of blood protons and reduce or eliminate the signal of the static background tissues. Suppose that a three-dimensional (3D) arteriogram could be acquired with MR, resulting in a 3D image with a positive intensity only in the arterial lumina larger than, for instance, ½ mm in diameter, and noise elsewhere. Such an image would consist predominantly of empty space, with the arteries taking up only a small fraction of the available volume. It seems wasteful to image all that static tissue in 3D only to have to cancel it out later.

From the NMR Unit, Baker 2, Department of Radiology, Massachusetts General Hospital, Boston, MA 02114, U.S.A. Address correspondence and reprint requests to Dr. V. J. Wedeen.

This work presents a geometrically efficient method for 3D vascular MR. The basic idea is that by reducing the imaging field of view, 3D vascular MR can be accomplished without sacrificing spatial resolution. Image aliasing or "wraparound" artifact is the usual result of a too-small field of view in MR, but this effect is innocuous with angiographic data: because the vascular tree is sparse, wraparound need not cause image overlap. Because the vascular tree is topographically connected, its image can be "unwrapped" to yield accurate vascular morphology at true scale.

THEORY

Data acquisition time is the nemesis of 3D MR imaging. Two geometric variables contribute to the MR image acquisition time: resolution and field of view (3). Field of view in Fourier transform (FT) MR imaging has a quite different meaning than it

does in conventional X-ray imaging. The output of an MR experiment should be described, not as a single image, but as an infinite array of copies of an image regularly spaced along a line. The width of the field of view determines the displacement between adjacent copies in this array. If the field of view is wider than the subject, its images appear widely separated. If the field of view is narrower than the subject, its images overlap, a phenomenon called aliasing or "wraparound." Each image coordinate has an independent resolution and field of view, but the phase-encoded coordinates are the focus of this discussion as they are rate limiting with conventional FT techniques. Routinely, MR imaging software displays a single rectangular image one field of view wide which has been extracted from this array. Hence, the full array can be restored by concatenating copies of this image.

Figure 1 illustrates the basic relationships between the pattern of phase-encoding gradient pulses, their intensity and number, and the image resolution and field of view. The spatial resolution of an image (in pixels per centimeter) is determined by the range intensities spanned by the gradient pulses. This corresponds to the height of the largest gradient pulse. The field of view (in centimeters) is inversely proportional to the intensity difference, i.e., the increment in magnitude, between consecutive gradient pulses. Intuitively, the intense gradient pulses probe the short wavelength features and determine the resolution, and the weak gradient pulses probe the long wavelength features and determine the field of view. When the size of the increment between gradient pulses is increased, a given range of gradient intensities is covered in fewer steps, and the field of view is reduced. Images with visible wraparound are said to have been "undersampled" because the increment between consecutive gradient pulses must have been too great, and the field of view too small for the subject under study.

Three-dimensional MR images are phase encoded in two dimensions and so a two-dimensional (2D) wraparound must be considered. In a 3D analog of Fig. 1 the copies of a 3D image are placed in a rectangular grid pattern (a lattice) on an infinite plane. The key observation for vascular imaging is this: If the 3D image is an angiogram, its copies in the grid pattern are unlikely to overlap each other even if the displacements between them are smaller than the diameter of the subject. Because the branch vessels are relatively thin and sparsely distributed, the images of the vascular tree can interdigitate without collision. As a result, a satisfactory 3D angiogram can be obtained with a 3D field of view only a fraction of the subject's size. The permissible field of view reduction is limited roughly by the aggregate cross-sectional area of the vessels. As noted, a reduced field of view shortens the data acquisition time pari passu. Because the vascular tree is topologically connected, it is simple to extract a single image of the vascular tree from the "forest" in the lattice of copies. This step may be automated by a surface detection program.

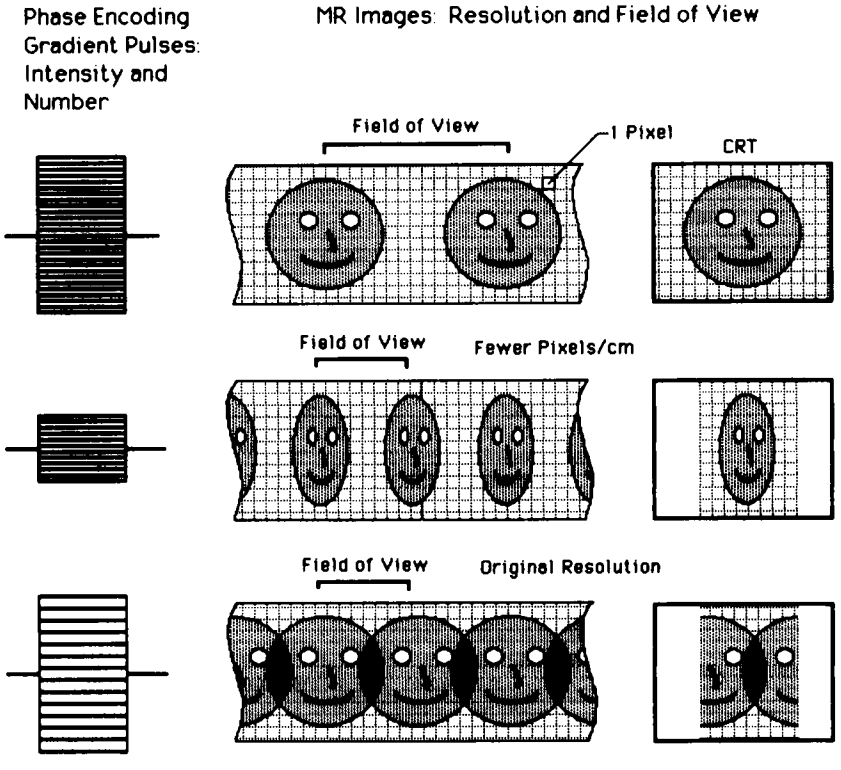

FIG. 1. Relationship between the number and intensity of phase-encoding gradient pulses (left column), image resolution, and field of view. The middle column is a schematic idealization of MR image data; right column shows the images as they appear on the CRT screen. The top row is a frame of reference. When the most intense gradient steps are deleted (middle row), the resolution (in pixels/cm) is reduced, but the field of view (in cm) is unchanged. When every second gradient pulse is eliminated (bottom row), the resolution is not affected (the pulse of maximal intensity has not changed), but the field of view is reduced. The undersampling caused by doubling the increments between gradients produces wraparound (aliasing) with overlap. Note that in all three cases, the entire volume of tissue is mapped on the CRT screen once.

MATERIALS AND METHODS

Imaging has been performed in a 1 m bore, 0.6 T commercially available imaging system. The imaging pulse sequence is shown in Fig. 2. This is the 3D analog of the flow imaging method previously described (1,4) in which the phase encoding is undersampled as discussed above. Electrocardiogram (ECG) gating is used to acquire a series of five 3D images interleaved at 175 ms intervals after the R-wave (such acquisitions have been called "multiphasic"). A maximum blood signal is obtained at this short repetition time (TR) (175 ms) by using a free induction decay–gradient echo pulse sequence and a low tip angle radiofrequency excitation determined by the Ernst equation (5). [The equilibrium signal is maximal when the tip angle ϕ satisfies the Ernst equation: $\cos(\phi) = \exp(-TR/T1)$. This gives $\phi \approx 30°$ for a TR = 175 ms and a T1 = T1 *blood* ≈1,000 ms (6).] Background suppression and flow contrast are accomplished by subtraction of any pair of these 3D images (as sets of complex numbers) because changes in arterial blood flow velocity affect the magnitude and the phase of the MR image data. (The first image in the series cannot be used for subtraction because it has a variable TR and consequently a T1 contrast different than the other images.) Depending on the physiology, different portions of the vascular tree may be seen with greater or lesser contrast when different pairs of images are subtracted. Averaging the difference images may provide more uniform and complete definition of the anatomy at a small cost in signal to noise. This process of acquisition and subtraction results in a single copy of the 3D arteriogram with manifold wraparounds. This 3D image is taken off-line for final processing.

Two additional processing steps are performed. First, the 3D arteriogram is duplicated N × N times in a rectangular lattice pattern (checkerboard), where N is the degree of geometric undersampling in each phase-encoded coordinate (subject diameter/field of view). Since the 3D image is actually one 3D field of view sliced from an infinite array of copies, duplication and catenation of these 3D images reassemble complete and uninterrupted copies of the vascular tree. Second, a surface detection program is initiated at the base of an arterial tree close to the center of the checkerboard and allowed to identify all the attached branches (Fig. 3 shows the 2D analog of this process). We have used a version of the popular solid-modeling program "Movie BYU" (Brigham Young University) that iteratively identifies voxels above a chosen threshold intensity which are adjacent to previously identified voxels and displays the result in 3D perspective. These perspective views of the arterial tree are the final image.

RESULTS

Figures 4–7 show the elements of a complete study. The acquisition is a study of the abdominal aorta of a normal volunteer. A conventional 2D projectional MR arteriogram (4 min study, coronal view; Fig. 4) was used for localization. The 3D data acquisitions used 32 × 32 = 1,024 phase-encoding

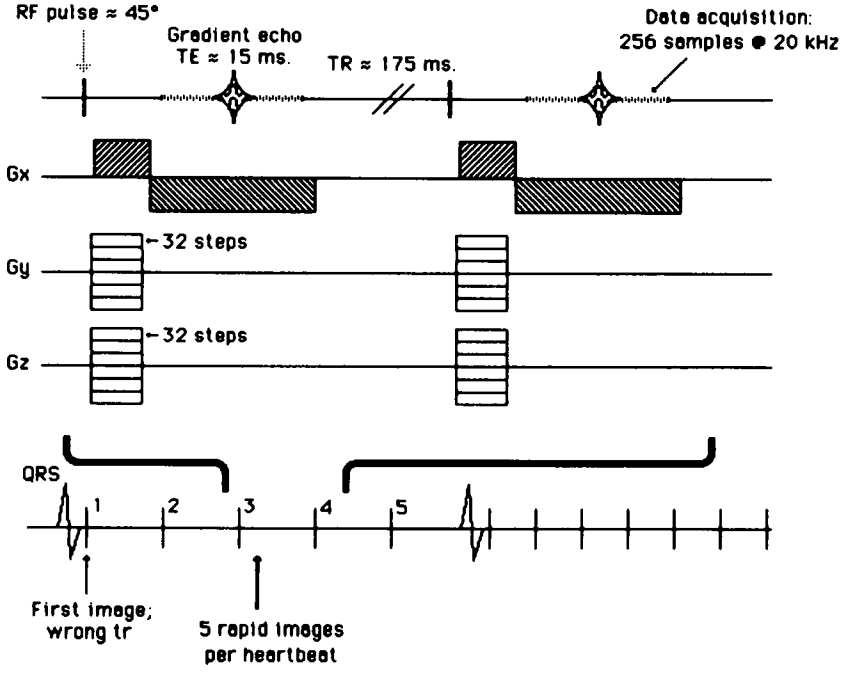

FIG. 2. Imaging pulse sequence with electrocardiogram-gating, three-dimensional (3D) Fourier transform spatial encoding (undersampling in *y* and *z*), and a gradient echo with a small tip angle radiofrequency (RF) excitation to minimize proton saturation. Each heartbeat triggers five sequential interleaved acquisitions at intervals of 175 ms. The echo time is 15.4 ms, and the readout gradient has an intensity of 0.14 G/cm, ~600 Hz/cm for protons.

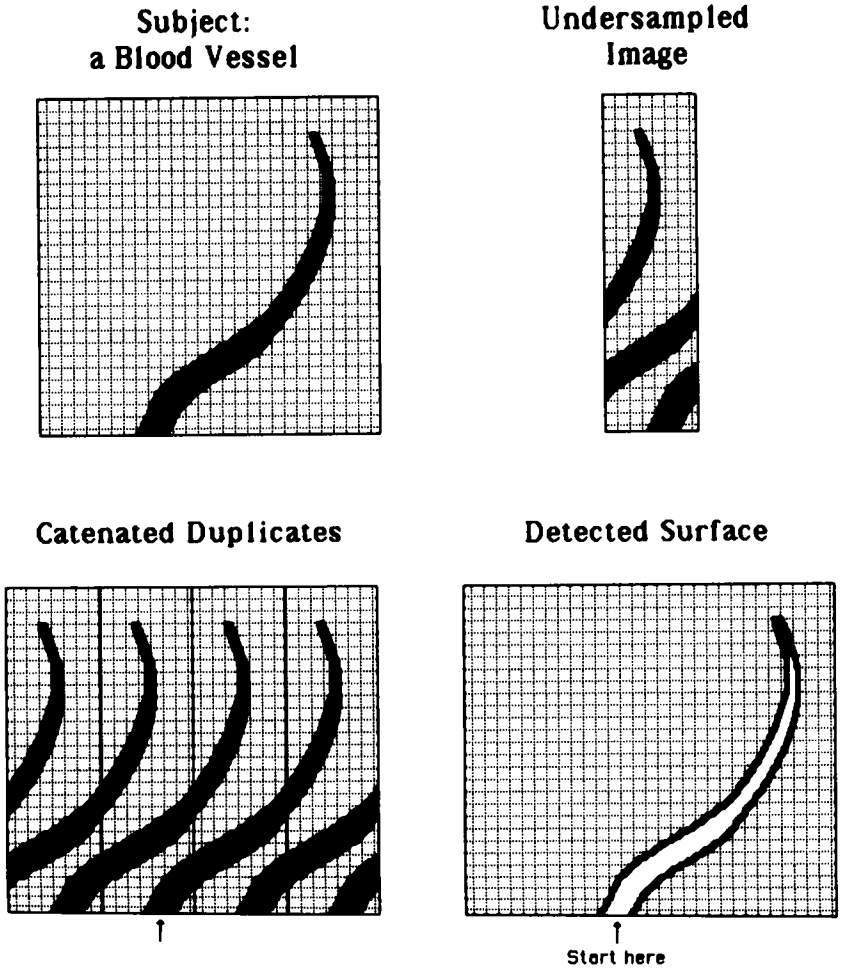

FIG. 3. Steps of image processing are illustrated in two dimensions. An artery (upper left) is imaged with a reduced field of view (upper right). In practice, this image would be the difference of undersampled systolic and diastolic images. The undersampled image contains precisely one copy of the artery but it is disconnected. The undersampled image is duplicated and catenated as shown, assembling complete and connected copies of the vessel (lower left). Surface detection identifies one copy of the vessel and restores true spatial relationships (lower right). Note that in 2D imaging, a branched vascular tree will overlap itself if field of view is substantially reduced.

FIG. 4. Conventional MR coronal projection arteriogram used for spatial localization. The pulse sequence is as shown in Fig. 2 except that the encoding in z has been omitted, and there is complete sampling and no reduction in field of view in y. With two signal averages, the acquisition requires 512 heartbeats or ~7 min.

steps to achieve a 1.6 × 2.4 × 2.4 mm voxel size (x, y, z, respectively) over a 40 × 7 × 7 cm field of view (256 × 32 × 32 voxels), with a wraparound of (4:1) × (4:1) = 16:1 in the y, z plane. The data acquisition required 1,024 heartbeats ≈16 min. Figure 5 shows stereo pairs of one prism of angiographic data, after subtraction, but prior to surface detection (image 4 minus image 3, having ECG gate delays of 525 and 350 ms from the R-wave, respectively). Catenation of four prisms of these data reassembles one complete copy of the aortic bifurcation and iliofemoral branches centrally, flanked by overlapping copies (Fig. 6). Perspective views of the aorta and common iliac arteries following surface detection are shown in Fig. 7.

DISCUSSION

Tomographic imaging is currently the predominant format in MR, evident victor of a competition that has included, among others, true 3D imaging. Three-dimensional imaging is based on the acquisition of a massive data set that simultaneously represents each small volume within the subject

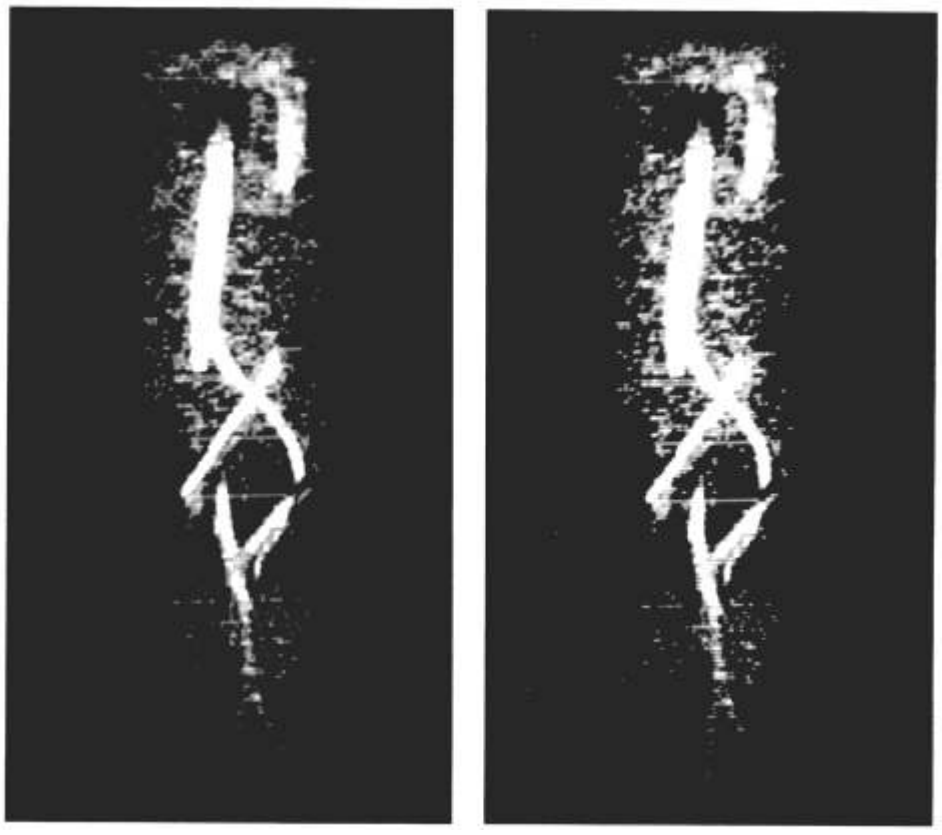

FIG. 5. Processing of a three-dimensional (3D) MR angiogram of the aortic bifurcation (image data immediately after subtraction). A threshold image intensity has been set at ~50% of the maximum blood signal intensity. Voxels having data values greater than or equal to threshold are shown in simulated 3D perspective on a vector graphics display screen. Aggregate data undersampling of 16:1 is the product of independent 4:1 undersamplings in *y* and in *z*. A stereo pair of one rectangular prism of data of 32 × 32 × 256 voxels is shown. The viewing angle corresponds to a left posterior oblique orientation. This stereo view helps emphasize that the noise is actually more rarified in 3D than in a two-dimensional projectional view. The arterial blood signal is on average 20 times as intense as the random noise and 5 times as intense as the unsuppressed background signal. This study did not use signal averaging.

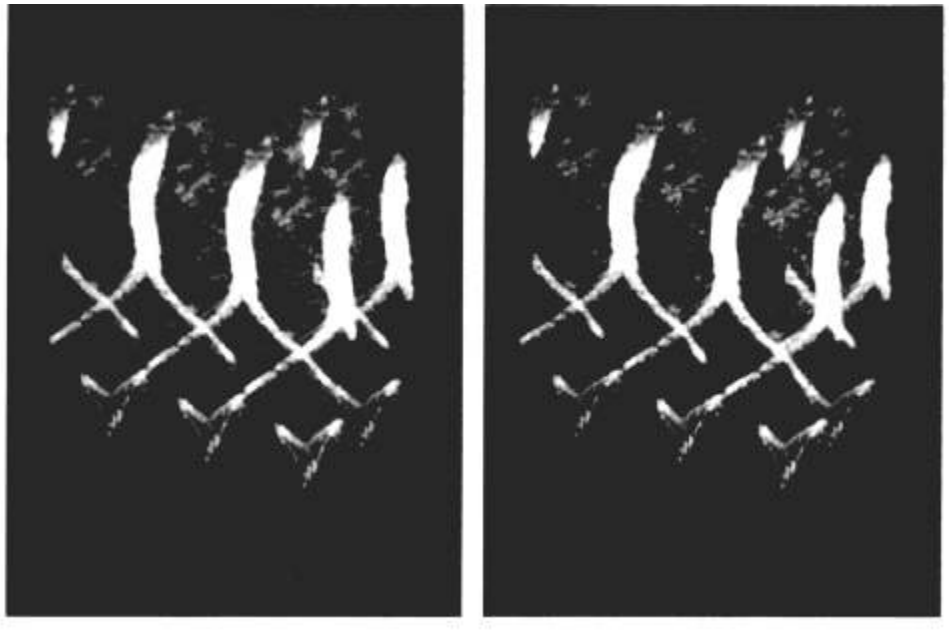

FIG. 6. Four copies of image data (the rectangular prism of Fig. 5) are catenated to reassemble one copy of the aortic bifurcation. In the actual image processing 16 such copies are catenated in a 4 × 4 grid pattern to accommodate the 16:1 data undersampling. The four copies shown here comprise an L-shaped subset of this grid.

FIG. 7. Following surface detection, a polygonal approximation of one copy of the aorta and common iliac arteries is shown in perspective. A solid appearance is created by shading that depends on the angle that each surface element presents to a hypothetical light source, positioned at upper right.

(voxel) with equal (isotropic) or nearly equal resolution in all three dimensions. The trouble with 3D imaging is the time it can take to acquire the data. In MR the jump from 2D to 3D typically squares number of steps needed for images with equal resolutions: a 128 step 2D image becomes a 16,384 step 3D image, and a 2 min scan becomes a 4 h impossibility. Nevertheless, the opportunity to see every point within the subject with equal fidelity and without bias in contrast or resolution defines an ideal toward which practical imaging methods must tend.

The invention of multislice tomography partially undercut the need for 3D imaging. Using stacked multislice data, investigators have used surface detection to define the chambers of the heart and the lumina of the great vessels of the chest and abdomen (7–9). It seems clear, however, that these methods are unreliable for the identification of vessels or pathology with dimensions much smaller than the slice thickness plus gap, typically ~1 cm. The current method enables the demonstration of vascular anatomy with isotropic resolution in 3D. Luminal morphology is defined with millimeter resolution in the great vessels, and it should ultimately be possible to identify with this technique vessels with diameter *less* than 1 pixel, as has been done in MR projection angiography (1–4).

It is important to note that this method of undersampling and geometric unwrapping is actually quite general. On the one hand, this method can dovetail with most forms of flow MR technique and, indeed, with all the methods that have been successful in projective MR angiography (2,10). On the other hand, more sophisticated 3D image processing techniques can be used. The current method for vessel identification by thresholding and surface detection has at least one clear drawback: Thresholding collapses the image's gray scale, represented by up to 16 bits in current imaging systems, down to 1 bit (above or below the threshold). Graphics faithful to the dynamic range of the data would facilitate quantitative flow measurements in a 3D setting and would probably provide a truer sense of vascular morphology as well (11).

The relationship between field of view reduction and the image signal-to-noise ratio should be briefly addressed. Field of view reduction in the phase-encoded coordinates causes no change in the recorded signal/gram of tissue and no change in the random noise per pixel compared with standard-field images with an equal number of RF pulses (12). To the extent that undersampling and wrap-around are tolerable on pictorial grounds, they permit the acquisition of equivalent signal in a fraction of the time. It is not clear at this point whether a similar conclusion will hold for the artifacts of respiration and peristalsis, which are partially coherent noise sources.

The need to avoid overlap between the copies of the vascular tree in the 3D image data is a serious challenge to this method. Vessel overlap will cause the surface detection routine to "spill" from one copy of the vascular tree to the next and opacify (by induction) some subarray of trees or the entire forest. The theoretical limit of undersampling is reached when the volume of the image matrix becomes as small as the net volume of the vessels (their "displacement"). This limit cannot be achieved in practice. How closely it can be approached depends on both the vagaries of vascular anatomy and our clinical intentions. If, for example, we wish to assess the morphology of a solitary vessel (e.g., the abdominal aorta), the field of view need be only marginally larger than the vessel's maximum cross section.

At this stage, a few recommendations can be made to help decrease the likelihood of overlap and the seriousness of its consequences. First, interfering structures can be excluded using thick slice or slab selection. For example, the right and left carotid arteries could be imaged separately in a multislice (multislab) acquisition. Second, structures with bilateral symmetry (e.g., renal arteries, aortic bifurcation) should be oriented asymmetrically in the image coordinates to avoid obligatory overlap. Phase variations of the blood signal may serve as a supplemental clue to the identities and locations of the vessels and partially mitigate the effect of overlap. With the present form of flow

contrast, the phase of the blood signal represents the sum of two influences: velocity-dependent phase shifts and position-dependent shifts of the background phase. Both types of phase shifts can cause destructive interference of signal where vessels collide, enabling such vessels to be distinguished. Recently, Dixon et al. have demonstrated a form of flow contrast in which blood signal is relatively free of velocity-dependent phase shifts (2). In this case variation of the background phase may help locate the vessel location in 3D as they observed in the context of projective imaging.

CONCLUSION

We have demonstrated a rapid and efficient method for obtaining a 3D MR image of a vascular tree. The basic notion of abbreviating imaging by undersampling and reassembly is quite general. It seems especially useful whenever the structure of interest has high contrast and is continuous and sparse. There would seem to be at least two good reasons for persuing 3D angiography with MR: morphology and physiology. Projective imaging gives an incomplete representation of vessel morphology, and biplane studies are only a partial solution. Although it is uncommon, biplane studies can be imprecise. Moreover, biplane images are costly. At a given resolution, 3D imaging must be evaluated as superior to projection imaging. As to physiology, it is well known that the sequence of flow disturbances in the progression of pathology is flow velocity first, pulse timing second, and flow volume third. At present, projective MR angiography has assured access only to the third of these parameters, equivocal access to the second, and none to the first. Three-dimensional methodology has the potential to provide the actual velocity distribution throughout the vessel, relative to the cardiac cycle. The spatial resolution of MR will not equal that of conventional X-ray studies in the near future. In consequence, the capability for velocity mapping may be the key to the competitive success of MR in vascular diagnosis.

Acknowledgment: Supported in part by NIH grant 1ROI HL37003-01. The authors are indebted to Byron Khors, Bill McCrosky, and Waldo Hinshaw of Technicare and Mark Handschumaker and Bill Carleson of the Massachusetts General Hospital Department of Cardiology for their indispensable help in the preparation of the graphics; to Bruce Rosen and Tom Brady for their continued encouragement and support; and to Lauren Abbate for her tireless technical assistance.

REFERENCES

1. Wedeen VJ, Meuli RA, Edelman RR, et al. Projective imaging of pulsatile flow with magnetic resonance. *Science* 1985;230:946–9.
2. Dixon WT, Du LN, Faul DD, Gado M, Rossnick S. Projection images of flowing blood labeled by adiabatic fast passage. *Magn Res Med* 1986;3:454–62.
3. Kumar A, Welti D, Ernst RR. NMR Fourier zeugmatography. *J Magn Res* 1975;18:69–83.
4. Meuli RA, Wedeen VJ, Geller SC, et al. Magnetic resonance gated subtraction angiography: lower extremities. *Radiology* 1986;159:411–8.
5. Ernst RR. Sensitivity enhancement in magnetic resonance. *Adv Magn Res* 1966;2:1–135.
6. Edelman RR, Wedeen VJ, Davis KR, Brady TJ. Multiphasic MRI of pulsatile CSF flow. *Radiology* (in press).
7. Axel L, Herman GT, Udupa JK, Bottomley PA, Edelstein WA. Technical note. Three-dimensional display of nuclear magnetic resonance (NMR) cardiovascular images. *J Comput Assist Tomogr* 1983;7:172–4.
8. Hale JD, Valk PE, Watts JC, et al. MR imaging of blood vessels using three-dimensional reconstruction: methodology. *Radiology* 1985;157:727–33.
9. Valk PE, Hale JD, Kaufman L, Crooks LE, Higgins CB. MR imaging of the aorta with three-dimensional image reconstruction: validation by angiography. *Radiology* 1985; 157:721–5.
10. Dumoulin CL, Hart HR. Magnetic resonance angiography. *Radiology* (in press).
11. Wedeen VJ, Rosen BR, Buxton R, Brady TJ. Projective MRI angiography and quantitative flow-volume densitometry. *Magn Res Med* 1986;3:226–41.
12. Hoult DI, Richards RE. The signal to noise ratio of the nuclear magnetic resonance experiment. *J Magn Res* 1976;24: 71–85.